

# The Effect of the Ball-Track Connection on the Energy Behavior of the Roller Gearing Gearbox

**Polák József László**

Széchenyi István University of Győr, Department of Road and Rail Vehicles  
Egyetem tér 1, 9026 Győr, Hungary; e-mail: polakj@ga.sze.hu

---

*Abstract: In this paper, I present an energetic study of the roller gearing gearbox by investigating the friction phenomena at the ball-track contact. The novelty of the subject is that the gearbox under investigation is a Hungarian invention, the energetic investigation of which has not been dealt with before. The study was carried out using a mathematical model based on analytical principles, in the course of which the principles and models used for ball bearings and ball screw drives were adapted and applied accordingly. It is important to mention that the study does not cover the complete gearbox, so losses outside the ball-race contact, e.g. bearing friction, seal friction, oil friction, air friction, etc., have not been considered in this paper.*

*Keywords: roller gearing gearbox; ball-track connection; rolling friction; coefficient of friction*

---

## 1 Introduction

In this paper, I present an energetic study of the roller gearing gearbox by investigating the friction phenomena at the ball-track contact. The energetic behaviour of gearbox used in engineering, and in particular in the automotive industry, is of great importance, and typically involves the identification of the sources of engine losses and their magnitude. This is particularly important in the case of electrically powered vehicles, as these losses have a significant impact on the vehicle's range, hence the importance of whether or not a gearbox is used in the design of an electrically powered vehicle and, if so, what its parameters are.

The novelty of the topic lies in the fact that the engine under investigation is a Hungarian invention, the energetic investigation of which has not been dealt with before. The roller gearing gearbox was invented by a Hungarian physicist [1] who wanted to use this type of action to transmit and modify rotary motion, since ball bearings only function as orienting, bedding components and are therefore not capable of modifying the rotary motion that passes through them, while spindle-

ball drives typically convert rotary motion into rectilinear motion, but none of them is directly suitable for transmitting and modifying rotary motion.

Figure 1 shows the physical model of the roller gearing gearbox under test. The gear can be defined as a dynamic system with three degrees of freedom since the balls in the connection are assumed to be elastic. The figure shows the general coordinates ( $q_1$ - $q_4$ ) that can be used to define the physical model of the gear.

The essence of the operation of the roller gearing gearbox is that ball(s) are used as transmission elements to transfer the movement and torque between the driving and driven wheels.

The ball enters the drive at a specific point and rolls into the converging grooves on the surface of the two discs. The groove transfers the drive from the driven wheel to the drive wheel through the wall. As the two discs rotate together, the ball travels along the grooves at their intersection point, and at the end of the grooves, the ball leaves the connection. Balls that are out of contact are guided back to the entry point on a leading path.

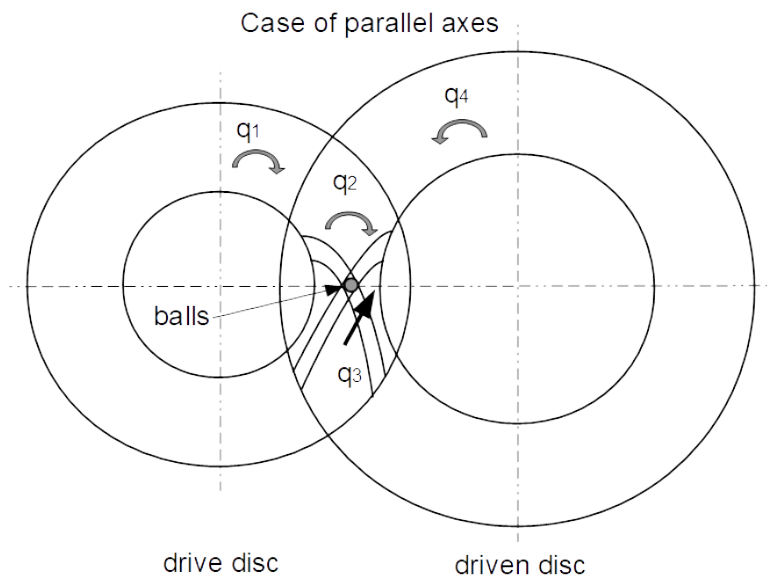


Figure 1

Physical model of the gearbox focused on the position and movement of the ball

The study was carried out using a mathematical model based on analytical principles, in the course of which the principles and models used for ball bearings and ball screw drives were appropriately adapted and applied. For these two machine elements, a very large literature has been produced on their motion, energetic behaviour and sizing, and this area is, therefore, highly researched.

However, it is important to note here that the working, loading and motion relations of the two machine elements are very similar, so that their mathematical modelling is broadly the same, while in the case of the roller gearing gearbox the ball-track relation is very similar to the previous one, but their motion characteristics with respect to each other are significantly different, which requires a modification of the relations applied to the previous cases.

In any case, it should be mentioned that the study does not cover the complete gearbox, so losses outside the ball-track relationship, e.g. bearing friction, seal friction, oil friction, air friction, etc., have not been considered in this paper.

In the case of an gearbox these losses are of great importance and play a key role in determining the total losses of the gearbox, but since in this article the ball-race contact is investigated, these losses have been neglected.

The total friction loss in a roller gearing gearbox includes the sliding and rolling friction loss in the ball-track contact and the friction loss in the return track, which is created between the balls and the return track. The friction loss in the system can be well described by some empirical relationships. These relations take into account the important parameters that are generated during the drive, such as load, rotation speed, lubricant, surface roughness, friction coefficient, etc. The relations describing this phenomenon require an accurate estimation of the friction forces and torques acting on the drive and driven rollers at the different working points.

In recent years, Hupert has developed simple and efficient computational procedures in the field of rolling bearings [2, 3]. And Olaru et al. have developed analytical models to determine the frictional forces generated during the operation of ball screw [4, 5]. The author has attempted to develop a new analytical model to determine the friction losses of roller gearing gearbox based on friction models of rolling element bearings and ball screw systems.

In the first part of the paper, the forces acting on the ball-track contact are presented, followed by the tangential forces and the geometric characteristics of the roller gearing gearbox that determine the friction losses of these gearbox. In the light of these, an analytical mathematical model is created to study the energetic behaviour of this gearbox through a specific concrete case.

## 2 Determination of the Forces Acting on the Ball

### 2.1 Determination of the Forces Acting on the Ball at the Contact Surface of the Ball Track

Figures 2, 3 show the forces acting on the balls in the x-z and x-y planes. By looking at the forces acting on the ball at the i-th point of the trajectory, it can be seen that between the groove wall of the driving disc and the ball, a force in the normal direction ( $F_{ni}$ ), perpendicular to the trajectory wall, and a force in the tangential direction ( $F_{ti}$ ), pointing in the direction tangential to the trajectory, are generated due to the driving force of the disc ( $F_{hi}$ ). As shown in the Figure 2, the normal directional force can be further decomposed into planar forces ( $F_{nixz}$ ,  $F_{nixy}$ ). The driving force on the groove wall can be determined from the torque of the driving motor ( $M_{mot}$ ) and the distance of the ball from the axis of rotation ( $r_i$ ) this force can be computed by relationship:

$$F_{hi} = \frac{M_{mot}}{r_i} \quad (1)$$

Knowing the driving force, the normal force between the ball and track can be determined on the basis of Figure 4 with the following relation:

$$F_{ni} = \frac{F_{hi}}{\cos \alpha \cdot \cos \beta} \quad (2)$$

Indexing i along the trajectory is necessary because the radius of the gear in the x-y plane, the radius of gyration ( $r_i$ ) and the radius of curvature of the trajectory depend on the position of the ball, and therefore vary continuously, unlike the case of rolling bearings or ball bearings, where the radius is the same along the entire trajectory of the motion.

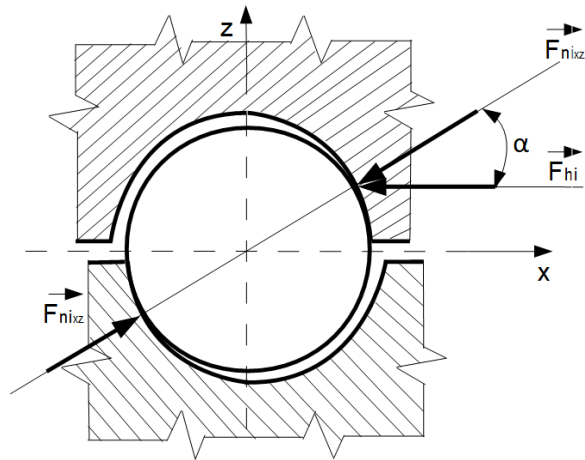


Figure 2  
Forces acting on a ball moving in track in the x-z

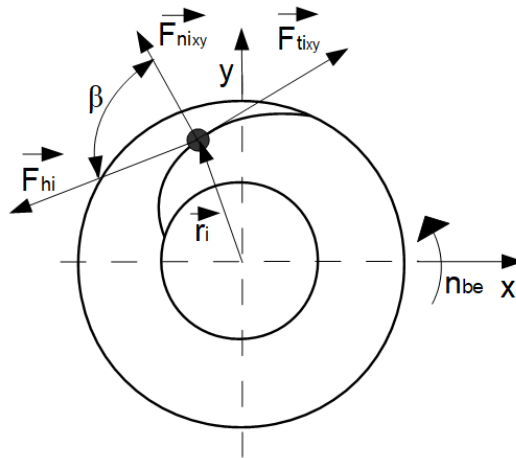


Figure 3  
Forces acting on a ball moving in track in the x-y

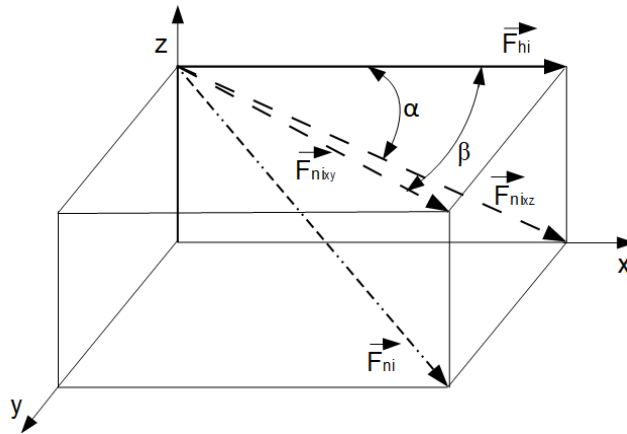


Figure 4

Determination of the spatial normal force ( $F_{ni}$ ) acting on the ball

## 2.2 Determination of Tangential Force at the Contact Surface of the Ball Track

The forces acting at the ball-track contact are: hydrodynamic rolling resistance force ( $F_r$ ), the force of pressure at the ball-track contact ( $F_{ni}$ ), the force of sliding ( $F_f$ ), the force of pressure between the balls ( $F_g$ ).

The hydrodynamic rolling force generates an EHD (elastohydrodynamic lubricating regime) lubrication condition at the contact surface by means of Poiseuille flow through the lubricant, which can be defined by the following relation [2, 4]:

$$F_r = 2,86 \cdot E \cdot Rx^2 \cdot k^{0,348} \cdot G^{0,022} \cdot U^{0,66} \cdot W^{0,47} \quad (3)$$

“where  $E$  [GPa] is the equivalent modulus of elasticity determined from the modulus of elasticity of the related materials,  $Rx$  [m] is the equivalent radius in the direction of rolling,  $k$  [-] is the ratio of the rolling radii,  $G$ ,  $U$ ,  $W$  [-] dimensionless material parameters, speed parameters and load parameters”.

In the case of a drive disk-ball connection:

$$\frac{1}{Rx1} = \frac{2}{d_w} - \frac{2 \cdot \cos \alpha}{d_m + d_w \cdot \cos \alpha} \quad (4)$$

In the case of a ball-driven disk:

$$\frac{1}{Rx2} = \frac{2}{d_w} + \frac{2 \cdot \cos \alpha}{d_m - d_w \cdot \cos \alpha} \quad (5)$$

Determination of the ratio ( $k$ ) of the rolling radii:

$$k = \frac{Ry}{Rx} \quad (6)$$

Determination of the transverse equivalent radius ( $Ry$ ):

$$Ry1 = \frac{f_1 \cdot d_w}{2 \cdot f_1 - 1} \quad \text{and the} \quad Ry1 = \frac{f_2 \cdot d_w}{2 \cdot f_2 - 1} \quad (7)$$

“where  $f_1$  and  $f_2$  are the curvature parameters for the drive disk and the driven disk, respectively, and  $d_w$  is the diameter of the ball”. Based on practical experience, the value of  $f$  generally varies between 0.515... 0.54 [5].

Definition of the material parameter ( $G$ ):

$$G = E \cdot \alpha_p \quad (8)$$

“where  $\alpha_p$  [GPa] is the piezoviscosity coefficient”.

Determination of the speed parameter ( $U$ ):

$$U = \frac{v \cdot \eta_0}{Rx \cdot E} \quad (9)$$

To determine the speed difference between the ball and the track, a new parameter, which is nothing but the internal gear ratio ( $i_{1b}$ ) must be introduced [6]. The internal gear shows how many turns the transfer ball makes per turns of the drive disk. The determination of the internal gear ratio can be determined as the quotient of the speed of the drive disc ( $n_1$ ) and the speed of the ball ( $n_b$ ):

$$i_{1b} = \frac{n_1}{n_b} \quad (10)$$

The speed of the drive disc can be clearly specified, while the speed of the ball must be determined. To determine the speed of the ball, the diameter of the ball ( $d_b$ ), the length of the path travelled by the ball, which can be determined by extracting from the geometric model the length of a path segment ( $l_1$ ) and the angular rotation of the drive disc ( $\alpha_1$ ) associated with the path segment Figure 5.

Using the parameters extracted from the model, you must first determine the number of turns of a ball ( $n_{b11}$ ) required to make a section of track with the following relation [6]:

$$n_{b11} = \frac{l_1}{d_w \cdot \pi} \quad (11)$$

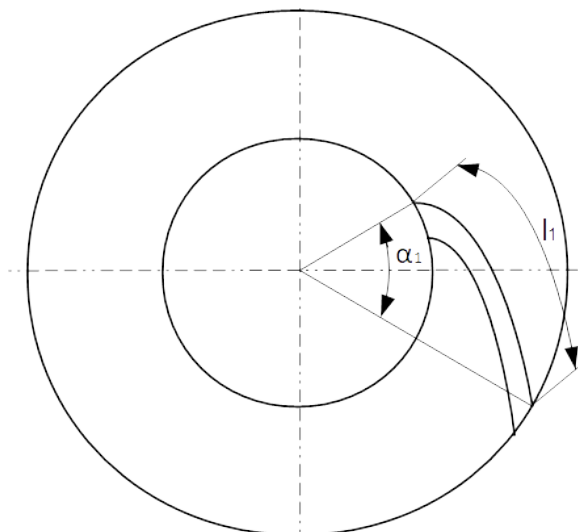


Figure 5

Length of a ball-track and associated rotation angle of the disc [6]

Once the ball speed required to complete a section of track has been determined, the ball speed per speed of the drive disk can be determined by dividing the  $360^\circ$  corresponding to one section by the angular rotation of the disk required to complete one section ( $\alpha_l$  [°]) and thus the value obtained shall be multiplied by the number of turns of the ball required to make a section of track [6]:

$$n_b = \frac{360^\circ}{\alpha_{l1}} \cdot n_{bt1} \quad (12)$$

If the ball speed ( $n_g$ ) is projected on one turn of the drive disk, the internal gear ratio is equal to the speed of the ball. Knowing the internal transmission ratio, the rotation of the ball can be determined by the following relation:

$$n_b = n_{mot} \cdot i_b \quad (13)$$

$n_{mot}$  is the speed of the drive motor, i.e. the speed of the drive disk. Using the parameters defined above, the speed difference between the ball and the track can already be determined:

$$v = n_b \cdot d_w \cdot \frac{\pi}{60000} \left[ \frac{m}{s} \right] \quad (14)$$

The load parameter ( $W$ ) can be determined by the following relation:

$$W = \frac{F_n}{E \cdot R x^2} \quad (15)$$



### 3 Torques at the Ball-Track Connection

The moment at the contact ellipse can be divided into two parts, the torque due to elastic deformation ( $T_{er}$ ) at the contact surface of the ball track and the frictional moment ( $T_f$ ) between the ball track and the ball.

The friction torque ( $T_f$ ) is due to the local shear stress ( $\tau$ ) between the contact surfaces, which can be determined by the following relation [2, 4]

$$T_f = \int \tau \cdot z \cdot dA = \int \mu \cdot p \cdot z \cdot dA \quad (16)$$

“where ( $z$ ) is the distance between the line of clean rolling and the position of the shear stress, ( $\mu$ ) is the local coefficient of friction, and ( $p$ ) is the local contact pressure”.

Assuming a Hertz pressure distribution and a constant coefficient of friction ( $\mu_m$ ), equation (16) can be approximated by the following equation [2, 4]:

$$T_f = 0,1 \cdot \mu_m \cdot \frac{F_n \cdot a^2}{Rd} \cdot (1 - 5 \cdot Y^3 + 3 \cdot Y^5) \quad (17)$$

“where  $Rd$  is the radius of deformation in relation to the ball-track;” and can be determined as follows:

$$R_d = \frac{2 \cdot d_w \cdot f}{2 \cdot f + 1} \quad (18)$$

in context (17),  $Y$  is a relative parameter that can be interpreted between the clean rolling point and the center of the contact ellipse.

To determine the major axis ( $a$ ) and minor axis ( $b$ ) of the contact ellipse, the length of the half-axes must be determined with the following approximations [2, 3]:

$$a \approx 1,552 \cdot R_x \cdot k^{0,4676} \cdot \left( \frac{F_n}{E \cdot R_x^2} \right)^{1/3} \quad (19)$$

$$b \approx 1,502 \cdot R_x \cdot k^{-0,1876} \cdot \left( \frac{F_n}{E \cdot R_x^2} \right)^{1/3} \quad (20)$$

“where  $T_{er}$  is the moment of elastic resistance in the case of clean rolling”; which can be determined by the relation of Snare [2, 3, 4]:

$$T_{er} = 7,48 \cdot 10^{-7} \cdot \left( \frac{d_w}{2} \right)^{1/3} \cdot F_n^{1,33} \cdot (1 - 3,519 \cdot 10^{-3} \cdot (k - 1)^{0,806}) \quad (21)$$

## 4 Friction Forces and Moments in Ball Track Contact

The total tangential force is the algebraic sum of the tangential contact forces in the rolling direction in the ball-track contact of the drive disc

$$F1 = \frac{T_{c1} + T_{c2} + T_{er1} + T_{er2} + T_b}{d_w} + F_{r1} + F_{r2} + \frac{(F_{r1} + F_{r2}) \cdot d_w \cdot \cos \alpha}{d_m} + \frac{F_i}{2} \quad (22)$$

Frictional torque generated at the ball-track contact of the drive disc:

$$Ts_1 = F1 \cdot R1 \quad (23)$$

“where  $R1$  is the rolling radius of the ball-to-track connection”:

$$R1 = \frac{d_{m1}}{2} + \frac{d_w \cdot \cos \alpha}{2} \quad (24)$$

“where  $d_{m1}$  is the mean value of the radius of the track of the drive disk in the x-y plane”.

The total friction moment for n balls is defined as the sum of the friction torques of the balls underload:

$$Ts_1 = \sum_1^n Ts_i \quad (25)$$

The total tangential force in relation to the ball track of the driven disk can be determined by vector algebraic summation of forces in the rolling direction:

$$F2 = \frac{T_{c1} + T_{c2} + T_{er1} + T_{er2} + T_b}{d_w} + F_{r1} + F_{r2} - \frac{(F_{r1} + F_{r2}) \cdot d_w \cdot \cos \alpha}{d_m} + \frac{F_b}{2} \quad (26)$$

Friction torque generated in relation to the ball-track of the driven disk:

$$Ts_2 = F2 \cdot R2 \quad (27)$$

“where  $R2$  is the rolling radius of the ball-to-track connection”:

$$R2 = \frac{d_{m2}}{2} + \frac{d_w \cdot \cos \alpha}{2} \quad (28)$$

“where  $d_{m2}$  is the mean value of the radius of the track of the driven disk in the x-y plane”.

The total friction torque on the driven disk tracks for n pieces balls can be determined as the sum of the friction torques of the balls under load:

$$Ts_2 = \sum_1^n Ts_{2i} \quad (29)$$

## 5 Estimation of Efficiency in the Tested Gearbox

When estimating the efficiency, sliding friction is neglected since pure rolling is assumed, and the efficiency can be described by the following relation:

$$\eta = \frac{T_{mot} - Ts_1 - Ts_2}{T_{mot}}. \quad (30)$$

## 6 The Results of the Study

A numerical program has been developed to analyse the variation of transmission friction torque and efficiency with drive motor torque.

The geometrical parameters used for testing the gearbox are given in the table 1.

Table 1  
The geometrical parameters used for testing the gearbox

No.	Parameters	Values
1.	ball diameter	$dw = 6 \text{ mm}$
2.	average radius of the tracks of drive disk in the x-y plane	$dm1 = 47.5 \text{ mm}$
3.	average radius of the tracks of driven disk in the x-y plane:	$dm2 = 65 \text{ mm}$
4.	total number of balls:	$Z = 86 \text{ pcs}$
5.	number of connected balls:	$z = 5 \text{ pcs}$
6.	contact angle:	$\alpha = 20^\circ$
7.	surface roughness of the ball:	$Rg = 0.6 \text{ }\mu\text{m}$ ,
8.	Surface roughness of the track of the drive and driven disk:	$Rt = 1.6 \text{ }\mu\text{m}$ ,
9.	coefficient of friction between balls:	$\mu b = 0.1$
10.	lubricant viscosity:	$\eta_0 = 0.1 \text{ Pas}$
11.	For the parameter $Y$ , it is assumed to be 0.34 for both the drive disc and the driven disc [7].	$Y=0,34$ ,
12.	the curvature parameters $f1$ and $f2$ for the drive disk and the driven disk are 0,53 [7].	$f1, f2=0,53$
13.	The drive motor torque was varied between 0... 100 Nm.	$T_{mot}=0\dots 100 \text{ Nm}$

Figure 6 shows that there is a small increase in efficiency in the initial stage ( $dM \approx 2 \text{ Nm} \rightarrow d\eta \approx 0.2\%$ ), which shows a monotonic decrease after tipping over ( $dM \approx 97 \text{ Nm} \rightarrow d\eta \approx 1.5\%$ ). Figure 7 shows that the friction torque increases slightly exponentially.

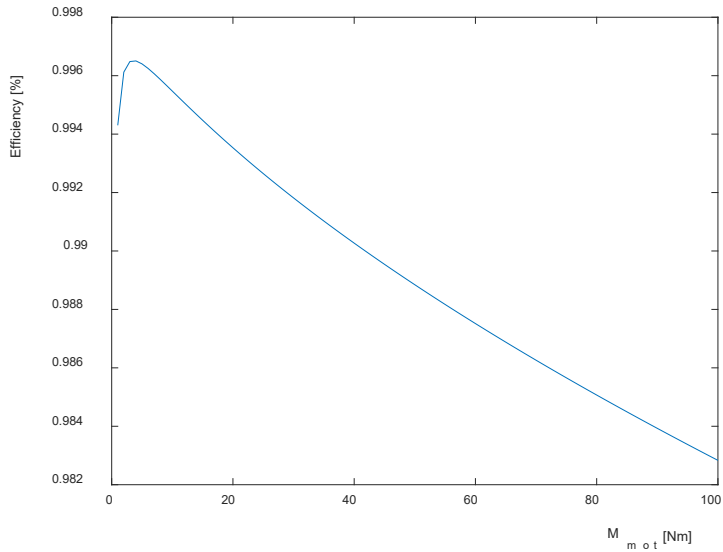


Figure 6

Variation in gearbox efficiency as a function of drive motor torque over the full operating range ( $M_{mot}=0 \dots 100$  Nm)

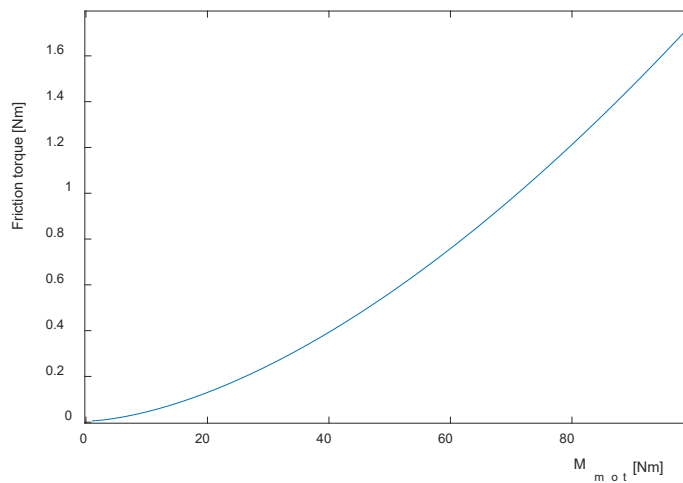


Figure 7

Variation of friction torque as a function of drive motor torque over the full operating range ( $M_{mot}=0 \dots 100$  Nm)

## 7 Investigation of Some Geometrical Parameters of the Roller Gearing Gearbox

In the case of a roller gearing gearbox, it is worthwhile to define the geometric parameters that affect the energetic behaviour of the gearbox over the full operating range, just as has been done for geared gearboxes.

When considering the geometric parameters of the gearbox, two geometric parameters seem to be of interest and importance, one is the ball diameter ( $d_w$ ) and the other is the average groove radius in the x-y plane ( $r_x$ ), as these are the parameters that typically determine the motion and loading conditions of the associated components. In addition to the two geometrical parameters, the viscosity of the lubricating oil ( $\eta$ ) used may also be of interest, as it has a significant effect on the friction generated during component contact, which is not negligible from an energy point of view, therefore, it is also worth investigating the lubricating oil viscosity.

Thus, the parameter vector of the roller gearing gearbox can be written as shown in the following figure:

$$\mathbf{p} = [d_w, r_x, \eta] \quad (1)$$

With the engine model and the selected parameters, a parameter sensitivity analysis can be performed.

In the first test, the ball diameter was varied by using four different ball diameters to investigate the variation in engine efficiency over the full operating range. The ball diameters were 1 mm, 3 mm, 6 mm, 9 mm.

The result of the run is shown in the Figure 8. From the obtained efficiency curves it is clear that the optimum ball size is not easy to determine, as the gearbox with small diameter balls ( $d_w=1\text{mm}$ , 3 mm) has a good efficiency in the initial stage but it deteriorates steadily with increasing load, probably due to the small surface area load transfer and the resulting overload.

As the ball size increases ( $d_w=6\text{ mm}$ ), the efficiency of the gearbox is worse in the initial low-load stage, but improves significantly in the higher load ranges, so this means that the energetically optimal behaviour (deformation, lubrication film) is obtained in the higher load ranges.

With a further increase of the ball size ( $d_w=9\text{ mm}$ ), the maximum efficiency does not increase, but the losses in the initial phase increase, so the tendency of the optimal ball size, i.e. to be smaller or larger, cannot be determined, but must always be determined according to the specific load conditions.

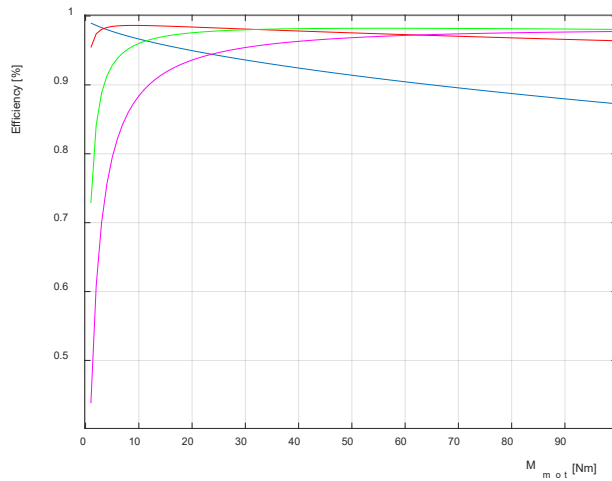


Figure 8

The effect of ball size variation on engine efficiency:  $n_{\text{mot}} = 1000$  rpm,  $M_{\text{mot}} = 1 \dots 100$  Nm  
 (blue line:  $d_w = 1$  mm, red line:  $d_w = 3$  mm, green line:  $d_w = 6$  mm, purple line:  $d_w = 9$  mm)

In the second test, the size of the radius in the x-y plane of the ball trajectory was varied by examining the variation of the engine efficiency over the full operating range for four different trajectory radii. The orbit radii were 10 mm, 50 mm, 100 mm, 150 mm.

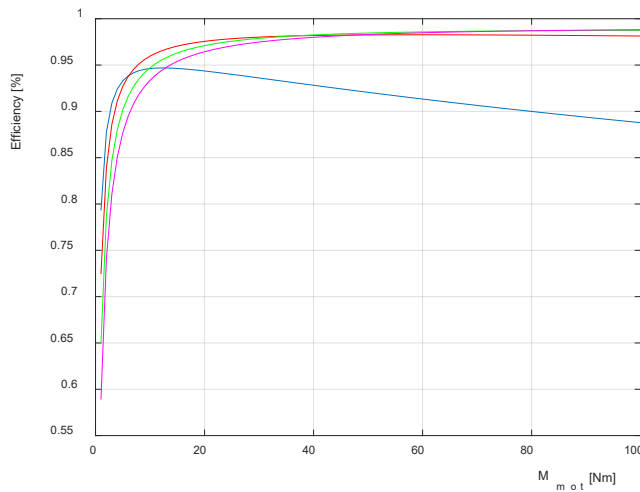


Figure 9

Effect of variation in the radius of the ball orbit in the x-y plane on the efficiency of the gearbox:  $n_{\text{mot}} = 1000$  rpm,  $M_{\text{mot}} = 1 \dots 100$  Nm (blue line:  $r_x = 10$  mm, red line:  $r_x = 50$  mm, green line:  $r_x = 100$  mm, purple line:  $r_x = 150$  mm)

The result of the run is shown in the Figure 9. From the efficiency curves obtained, it is clear that the optimum orbit radius cannot be determined in general since apart from the smallest radius ( $r_x=10$  mm) orbit, there is no significant variation in the efficiency of the gearbox for the other three orbits over the whole operating range, so the optimum size can be determined according to the load conditions.

In the third test, the dynamic viscosity of the lubricating oil used was varied by testing the change in engine efficiency over the full operating range with four different viscosities of oil. The selected oil viscosities were as follows: 0,1 Pas; 0,3 Pas; 0,6 Pas; 1,0 Pas.

The result of the run is shown in the following figures (Figure 10, Figure 11). Examining the first diagram, it appears as if there is a single efficiency curve on the diagram, so it was necessary to draw the second diagram, which zooms in on the near-horizontal section of the diagram, from which it can be seen that the change in lubricating oil viscosity has a very minimal effect on engine losses, and therefore further investigation is negligible from this point of view.

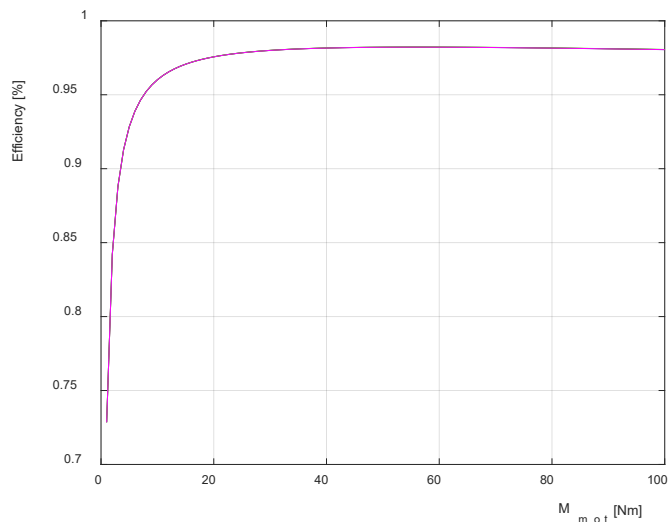


Figure 10

Effect of lubricating oil dynamic viscosity variation on engine efficiency:  $n_{mot}=1000$  rpm,  $M_{mot}=1 \dots 100$  Nm (blue line:  $\eta=0,1$  Pas, red line:  $\eta=0,3$  Pas, green line  $\eta=0,6$  Pas, purple line:  $\eta=1,0$  Pas)

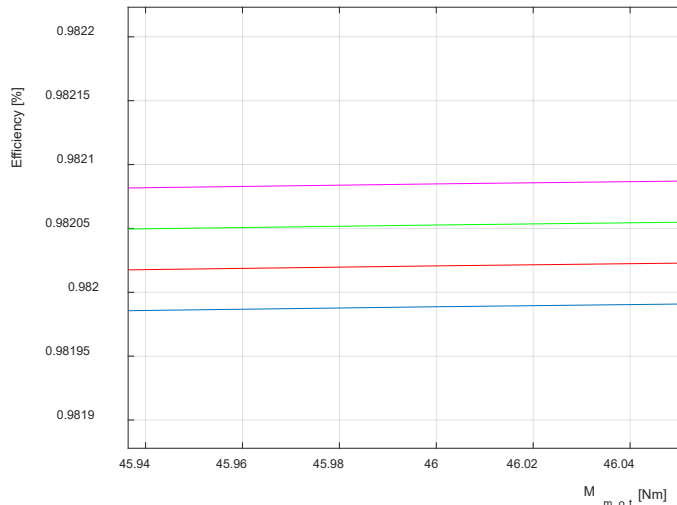


Figure 11

Effect of lubricating oil dynamic viscosity variation on engine efficiency:  $n_{mot}=1000$  rpm,  $M_{mot}=1 \dots 100$  Nm (blue line:  $\eta=0,1$  Pas, red line:  $\eta=0,3$  Pas, green line  $\eta=0,6$  Pas, purple line:  $\eta=1,0$  Pas)

## Conclusion

Based on the balance of forces and torques acting on the ball, the rolling friction forces between the discs and the balls are determined by the shear stress at the contact surfaces. The frictional force includes the rolling friction force, which was determined by considering two components, the moment due to elastic deformation and the frictional moment between the ball and the track.

By summing the sliding and rolling resistance of the contact ellipse, we obtain the force and torque acting on the discs for the case of a contact ball. Extending the contact of one ball to all balls in contact gives the total frictional torque on the discs.

The results obtained by the model are realistic based on the results presented in the literature on systems operating on similar principles.

Several simplifications have been made in the construction of the mathematical model created, these simplifications were mainly made in the definition of some geometric parameters, such as the average radius of the trajectories of the driving and driven discs in the x-y plane, which negatively affects the accuracy of the model, therefore, the model needs further refinement, which will be carried out in the near future.

The analytical procedure used in this paper is an improvement of the modelling procedure used by our department in previous papers [8, 9, 10, 11, 12, 13].



## Acknowledgment

The research was supported by the Ministry of Innovation and Technology NRDI Office within the framework of the Autonomous Systems National Laboratory Program.

## References

- [1] Dr. Pál Bogár, Bearings for Gearings presentation, International Conference on Gears, 2015 october5-7, pp. 115-126, 11p.
- [2] HOUPERT, L., “Numerical and Analytical Calculations in Ball Bearings”, Proc. of Congres Roulements, Toulouse, 5-7 Mai (1999), pp. 1-15
- [3] HOUPERT, L., “Ball Bearing and Tapered Roller Bearing Torque: Analytical, Numerical and Experimental Results”, Proc of STLE Annual Meeting, Houston, May 19 – 23, 2002
- [4] OLARU, D.N., LORENZ, P., RUDY, D., CRETU, SP., PRISACARU, GH., “Tribology Improving the Quality in the Linear Rolling Guidance Systems”, Part 1- “Friction in Two Contact Points Systems”, Proc. of the 13th International Colloquium on Tribology, Esslingen (Germany), 15-17 January, 2002
- [5] OLARU, D. N., P.LORENZ, D. RUDY, “Friction in the Circular – Arc Grooves Linear Rolling Guidance System”, Tribologie und Schmierungstechnik, 2 (2004), pp. 9 –14
- [6] Péter Öri, József Polák, The research of the static and dynamic characteristics of the components of the roller gearing gearbox in order to determine the strength dimensioning, XIII. IFFK 2019, Budapest, 2019. August 26- 29, Paper 29
- [7] Dumitru Olaru, George C. Puiu, Liviu C. Balan, Vasile Puiu, A New Model to Estimate Friction Torque in a Ball Screw System, in book: Product Engineering, January 2005
- [8] Dr. István Lakatos, Valve timing of vehicle engines, Győr, Hungary: Jaurinum Bt. (1994) , 132 p.
- [9] Lakatos, István, Engine power measurement in stationary operating condition on a roller vehicle brake pad, MicroCAD 2010: XXIV. microCad International Scientific Conference: Section E: Materials Science and Technology, Miskolc, Hungary: University of Miskolc (2010) pp. 33-38, 6 p.
- [10] Dániel, Pup; Ádám, Titrik; Ferenc, Szauter; László, Bisits, Fitting and optimizing an intelligent electric powertrain into an existing city vehicle, OGÉT 2013 XXI International Mechanical Engineering Meeting, Cluj-Napoca, Romania: Hungarian Technical Scientific Society of Transylvania (EMT) (2013) pp. 330-333., 4 p.

- [11] István, Lakatos, Ádám, Titrik, DETERMINATION OF POWER AND TORQUE CURVES OF VEHICLES BASED ON DIAGNOSTIC METHODS, Proceedings of the 12th International Conference on Heat Engines and Environmental Protection, Budapest, Magyarország : Budapest University of Technology and Economics, Department of Energy Engineering (2015), pp. 43-49, 7 p
- [12] Tamás Péter; István Lakatos; Ferenc Szauter, Analysis of the Complex Environmental Impact on Urban Trajectories, ASME 2015 International Design Engineering Technical Conferences and Computers and Information in Engineering Conference: Mechatronics for Electrical Vehicular Systems, New York (NY), Amerikai Egyesült Államok: American Society of Mechanical Engineers (ASME) (2016) Paper: DETC2015-47077; V009T07A071, 7 p.
- [13] Hegyi, N., & Jósvai, J., Hazardous Situations and Accidents Caused by Light and Medium Unmanned Free Balloon Flights. *Acta Technica Jaurinensis*, 2020, pp. 295-308, 13p.